Modeling of the Flow Properties and Discharge of Halon Replacement Agents

P.J. DiNenno, E.W. Forssell, M.J. Ferreira, C.P. Hanauska, and B.A. Johnson

Hughes Associates, Inc.
6770 Oak Hall Lane, Suite 125
Columbia, Maryland 21045
(301) 596-2190
FAX (301) 596-2295

1 Introduction

The phaseout of halons and the rapid introduction of a wide range of halocarbon-based fire suppression agents have forced the development of flexible theoretically-based engineering models of the two-phase flow behavior in piping. Existing methods primarily used for Halon 1301 were generally proprietary and primarily empirically based and subject to certain constraints and limitations [1]. There was a clear need to develop a flow calculation program which could be readily adapted for new agents and could calculate the flow characteristics of fire suppression agents across the wide range of real engineering systems in reasonable time scales.

The flow program described is capable of predicting the two-phase flow characteristics of halon replacement agents based on their thermodynamics properties. The program has been tested against six different agents and agent blends. It is designed to be readily adopted to both new agents and manufacturers hardware.

Since the program continues to be improved and modified for an increasing range of agents, this documentation should be viewed as an approximate guide to the algorithms utilized.

2 Theory/Model Description

In 1984, Elliot et al., at the Jet Propulsion Laboratory, developed a simplified model for Halon 1301-nitrogen discharges based on their experience with steam-water-air mixtures [2]. However, their model, HFLOW, was limited to single nozzle systems or multi-nozzle systems that could reasonably be resolved to single nozzle systems. Spurred by the success of HFLOW, the present model incorporates many of the assumptions and concepts used in HFLOW while extending the model to more general application and to the discharge flows of a range of halon alternatives.

In HFLOW and the present model, two basic simplifying assumptions are made. First, it is assumed that the conditions in the cylinder (pressure, temperature, and composition) are solely functions of the initial conditions and the outage fraction (fraction of the initial charge mass having left the cylinder). This assumption effectively ignores the

impact of the increased kinetic energy of the fluid leaving the cylinder on the cylinder energy balance. The second assumption is that of quasi-steady flow, i.e., the average flow rate over a small timestep is equal to the flow rate that would exist if the cylinder conditions were held steady during that time step.

The flow of the agent through the pipe network is handled in an iterative fashion. A flow rate is estimated, and the network is stepped through to determine the conditions at the nozzle. The pressure and temperature at each node in the network are determined by solving both momentum and energy balances. The branches in the network are actually stepped by 34.5 kPa (5 psi) pressure drops with the distance traveled determined through the momentum balance (the pressure increment is adjusted so that nodes are met within 8 cm (3 in.)). This is done to ease the identification of sonic conditions in the pipe, i.e., if sonic conditions are encountered, the travel distance is zero. The estimated flow rate is then refined by comparison to the determined flow through the nozzles and the process repeated. The elapsed time is then determined by a mass balance, i.e., the mass having left the cylinder divided by the determined mass flow rate. The heat transferred from the pipe walls to the flowing fluid is assumed to be insignificant. The flow through the pipe network is also assumed to homogeneous (liquid and vapor travels through the network at nominally the same velocity with one phase evenly dispersed in the other).

Phenomenologically, the discharge flow is divided into five sections as shown in Figure 1, and the relationship between mass flow rate leaving the cylinder and the mass flow rate through the nozzles is adjusted accordingly. In the first section, pipe filling, the agent has not yet reached the nozzles and progresses through the network at sonic conditions. In the second section, the pressure and mass in the pipe network builds to a peak value. During this section, the flow rate through the network drops while the flow rate through the nozzles increases. The increased mass in the network is therefore equal to the product of the time increment and the difference between the flow rate leaving the cylinder and the flow rate through the nozzles. During the third section, between the achievement of the pipe peak pressure and when the cylinder runs out of liquid, the mass flow rate out of the cylinder is equal to that out the nozzles. After the cylinder runs out of liquid, the vapor front moves through the network in a manner similar to that of the liquid front during pipe filling except that the flow of the liquid out of the nozzles determines the flow rate and in general keeps the vapor flow rate low. After the nozzles are cleared of liquid, the flow rate out of the cylinder increases dramatically at first and then falls off. During this final section, the mass flow out of the cylinder is once again equal to the flow rate through the nozzles. If the cylinder runs out of liquid prior to the achievement of the pipe peak pressure, the nozzle pressure may in fact continue to rise, but the apex will not be as high as it would have been otherwise. and the "steady" liquid flow section never occurs. Another deviation occurs if the nozzles do not control the flow rate or completely control the flow rate. In the extreme, this causes the pipe peak pressure to have already occurred when the liquid front reaches the nozzles, and the second section is skipped. The overall structure of the model is diagramed in Figure 2

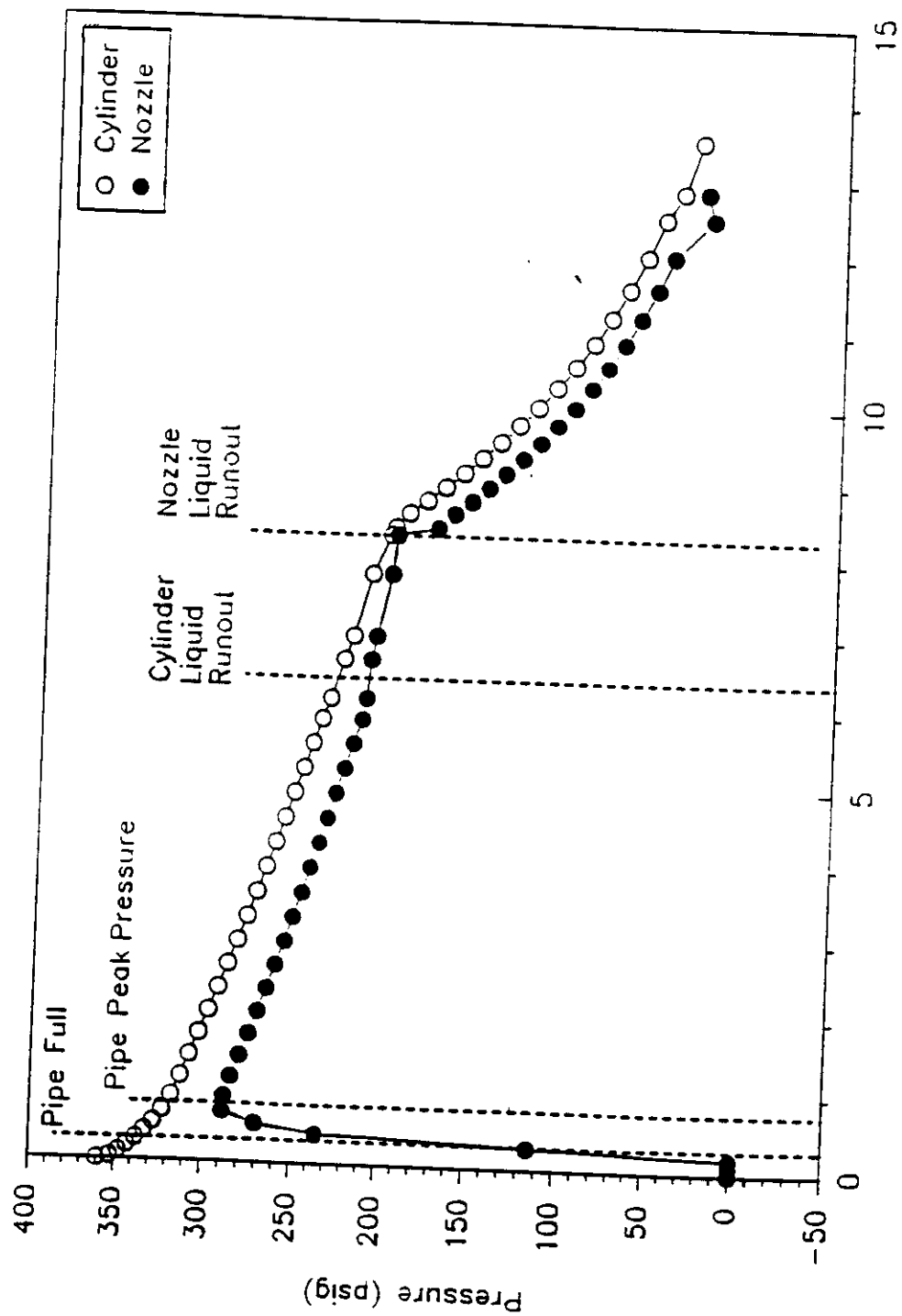

Figure 1 Discharge Flow Phenomenon

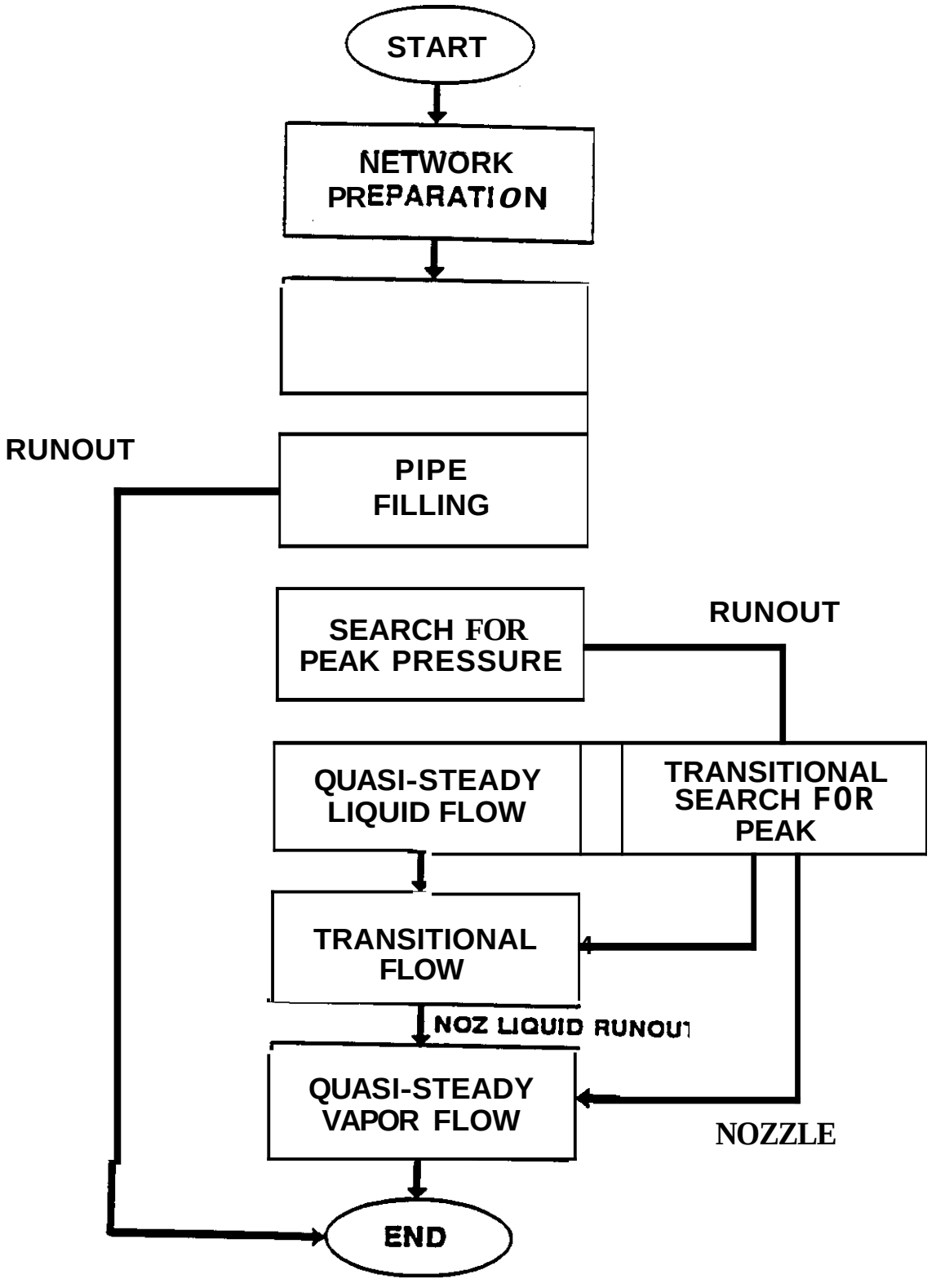

Figure 2. Flow Program Organization

3. Governing Equations

With the assumptions of adiabatic expansion and insignificant kinetic energy changes, the conditions at the cylinder are determined by stepping down the cylinder pressure by increments of 34.5 kPa (5 psi). The mass having left the cylinder, M_{loss}, being determined from the volume of the fluid at the end of the pressure increment as follows:

$$\begin{aligned} Vol_{loss} &= Vol_{fluid} - Vol_{cyl} \\ M_{loss} &= Vol_{loss} \cdot \rho_{loss} \end{aligned} \qquad (1)$$

where Vol_{loss} is volume of the fluid that left the cylinder during the pressure interval, V_{fluid} is the total volume occupied by the mass that was in the cylinder at the beginning of the interval at the pressure and temperature at the end of the interval, Vol_{cyl} is the volume of the cylinder, and ρ_{loss} is density of the fluid that left the cylinder (equal to the vapor density after liquid run out and equal to the liquid and bubble average density before liquid run out).

The temperature at the end of the increment is determined from an energy balance, i.e., the change in internal energy in the cylinder is off set by the enthalpy leaving with the departing fluid as follows:

$$M_1 u_1 - (M_1 - M_{loss})\, u_2 = M_{loss} H_2 \qquad (2)$$

where M_1 is the mass in the cylinder at the beginning of the interval, H_2 is the specific enthalpy of the fluid leaving the cylinder, u_1 and u_2 are the internal energies of the fluid in the cylinder at the beginning and the end of the pressure step. The heat transferred from the cylinder walls to fluid inside and the kinetic energy increase in the departing fluid are assumed to be insignificant.

The related continuity, momentum and energy equations for the flow through a branch with adiabatic flow are as follows:

$$\begin{aligned} V_{out} &= V_{in} \left(\frac{\rho_{in.,ave}}{\rho_{out,ave}} \right) \\ DP &= \rho_{ave} V_{ave} (V_{in} - V_{out}) + \rho_{ave} g (z_{in} - z_{out}) + DP_f \\ (h_{out} - h_{in}) &= 0.5 (V_{in}^2 - V_{out}^2) + g (z_{in} - z_{out}) + \frac{DP_f}{\rho_{ave}} \end{aligned} \qquad (3)$$

where DP is the total pressure drop in the branch, p is the density, g is the acceleration due to gravity, V is the velocity, z is the elevation, h is the specific enthalpy, and DP, is the pressure drop due to friction. Several two-phase flow friction loss formulations have been implemented and tested. With the assumption of homogeneous flow, the pressure drop due to friction is estimated using average properties as follows:

$$DP_f = \frac{\rho_{ave} f L V_{ave}^2}{(2D)} \quad (4)$$

where D is the diameter of the pipe, and f is the friction coefficient which for high reynolds flows reduces to only a function of the equivalent sand roughness to pipe diameter ratio [5].

In practice, the momentum balance is solved for the pressure drop due to friction and substituted in the energy balance, which leads to the following pair of equations that are solved for the travel distance, DL, during a given pressure increment:

$$(h_{out} - h_{in} = 0.5 (V_{in}^2 - V_{out}^2) - V_{ave} (V_{in} - V_{out}) - \frac{DP}{\rho_{ave}}$$

$$DL = \frac{DP - \rho_{ave} V_{ave} (V_{in} - V_{out})}{\frac{\rho_{ave} g (z_{in} - z_{out})}{L_{eq}} + \frac{DP_f}{DL}} \quad (5)$$

where L_{eq} is the total equivalent length of the branch. note that DL is increments of equivalent length rather than actual length.

Flow through the nozzle is handled in a similar manner to flow through the pipe network, i.e., a pressure increment is stepped down with the velocity increase, assuming isentropic expansion, and the mass flow rate using the effective nozzle orifice area are determined. The actual mass flow rate if the maximum calculated flow rate over a pressure increment. The energy, entropy and orifice equations are as follows:

$$(h_1 - h_2) = 0.5 (V_2^2 - V_1^2)$$

$$(V_2^2 - V_1^2) = 2 \left(\frac{MF_V}{\rho_{V,ave}} \log \left(\frac{P_1}{P_2} \right) + \frac{MF_L (P_1 - P_2)}{\rho_{L,ave}} \right) \quad (6)$$

$$m = \rho_{2,ave} A_o V_2$$

where MF_V and MF_L are the mass fractions of the vapor and liquid respectively. Note that the entropy balance is approximated by treating the vapor as an ideal gas and the liquid as incompressible [2].

The determination of the elapsed time is accomplished through a mass balance:

$$t = \frac{m_{loss}}{m_{t,cyl}}$$

$$t = \frac{M_{loss} - (M_{pipe,1} - M_{pipe,2})}{m_{t,noz}} \qquad (7)$$

$$t = \frac{M_{pipe,2} - M_{pipe,1}}{m_{t,cyl} - m_{t,noz}}$$

where $m_{t,cyl}$ and $m_{t,noz}$ are the total flow rates out of the cylinders and nozzles, $M_{pipe,1}$ and $M_{pipe,2}$ are the mass stored in the pipe at the beginning and end of the time interval. Which version of the mass balance or combination of mass balances used depend on the region of the discharge. The first version is used until the liquid front reaches the nozzles. Between liquid full and the pipe peak pressure is reached, the mass flow from the cylinder is determined from the last version of the mass balance with the elapsed time determined from the first if cylinder liquid runout does not occur or until it occurs and second version if it has occurred. During the remaining flow sections, the second version of the mass balance is utilized.

During the transitional flow between cylinder liquid runout and nozzle liquid runout, the liquid/vapor interface is moved through the network with the volumetric flow rate being the same on both sides. The temperature on the liquid side of the interface is solved for with a simplified energy balance between the last cylinder step prior to liquid runout and conditions at the interface:

$$H_{cyl} - H_{int} = \frac{V_{int}^2 - V_1^2}{2g}$$

$$V_1 = \frac{P_{int} V_{int}}{P_{cyl}} \qquad (8)$$

4. Thermodynamic Property Prediction

The thermodynamic properties required in the equations previously presented, were determined from least square curve fits to the basic correlations developed by Elliot et al. [2] for use in HFLOW. The thermodynamic data for alternative gases for use in these correlations, was taken from the literature values (Wilson et al.) [6]. Unavailable thermodynamic properties for certain halon alternative nitrogen mixtures were estimated using the Soave-Redlich-Kwong equation of state [7,8]. The vapor specific volume, v, of nitrogen is determined using the original version of the Redlich-Kwong [2,7].

$$P = \frac{RT}{MW\,(v+b)} - \frac{a}{t^{0.5}\,v\,(v+b)}$$

$$a = \frac{0.42728\,R^2\,T_c^{2.5}}{P_c} \qquad (9)$$

$$b = \frac{0.08664\,RT_c}{P_c}$$

where R is the ideal gas law constant, MW is the molecular weight, T_c is the critical temperature, and P_c is the critical pressure.

The saturated vapor specific volume of the agent is estimated from a curve fit of utilizing a compressibility term:

$$ZMW = \frac{Pv}{RT} \qquad (10)$$

$$ZMW = C_{1,1} + C_{1,2}\,(T - T_o) + C_{1,3}\,(T - T_o)^2 + C_{1,4}\,(T - T_o)^3$$

where Z is the saturated vapor compressibility and T_0 is reference temperature **273.15** K **(491.7°R).**

The saturated liquid density of the agent was estimated from the following curve fit:

$$\rho_l = C_{2,1} + C_{2,2}\,(T_c - T) + C_{2,3}\,(T_c - T)^{0.5} + C_{2,4}\,(T_c - T)^{0.33} + C_{2,5}\,(T_c - T)' \qquad (11)$$

where T_c is the agent critical temperature.

The saturated agent enthalpy was curve fit to the following equations:

$$H_l = C_{3,1} + C_{3,2}\,(T - T_o) + C_{3,3}\,(T - T_o)^2 + C_{3,4}\,(T - T_o)^3$$

$$H_v = C_{4,1} + C_{4,2}\,(T - T_o) + C_{4,3}\,(T - T_o)^2 + C_{4,4}\,(T - T_o)^3 \qquad (12)$$

where H_l and H_v are the specific liquid and vapor enthaplies of the agent and T_0 is reference temperature **273.15** K **(491.7R).**

The specific enthalpy of nitrogen as a vapor was correlated with the following equation:

$$H_N = C_{5,1} P + C_{5,2} (T_a - T) + C_{5,3} P (T_a - T) + C_{5,4} P (T_a - T)^2 \quad (13)$$

where H_N is the nitrogen enthalpy and T_a is ambient temperature (300 K or 540°R). The enthalpy of solution was assumed to be insignificant (enthalpy of the nitrogen vapor=enthalpy of the dissolved nitrogen).

The agent vapor pressure was correlated through the following equation:

$$\log_{10} P_v = C_{6,1} + \frac{C_{6,2}}{T^2} + \frac{C_{6,3}}{T} + C_{6,4} T + C_{6,5} T^2 \quad (14)$$

The additional liquid volume due to dissolved nitrogen was correlated through the following equation

$$V_{l,n} = C_{7,1} - C_{7,2} Ln (T_c - T) \quad (15)$$

where T_c is the agent critical temperature.

The composition of both phases was correlated through the Henry's Law coefficient:

$$Hen = \frac{P_N}{x_N} = \frac{P - 1 (1. - x_N) P_v}{x_N} \quad (16)$$

$$Hen = C_{8,1} + C_{8,2} (T - T_o) + C_{8,3} (T - T_o)^2 + C_{8,4} (T - T_o)^3$$

where Hen is the Henry's Law coefficient, P_N is the nitrogen partial pressure, x_N is the mole fraction of nitrogen in the liquid phase and T_o is the base temperature 255.3 K (459.6 R).

The constants generated for these equations are given in Table 1 and have been tested against experimental or SRK estimated values.

Table 1. Thermodynamic Constants (Predicted or Experimental)

Equation	Constant
Nitrogen Specific Volume, v_N	a b
Agent Vapor Compressibility, ZMW	$C_{1,1}$ $C_{1,2}$ $C_{1,3}$ $C_{1,4}$
Agent Liquid Density, ρ_l	$C_{2,1}$ $C_{2,2}$ $C_{2,3}$ $C_{2,4}$
Agent Liquid Enthalpy, H_l	$C_{3,1}$ $C_{3,2}$ $C_{3,3}$ $C_{3,4}$
Agent Vapor Enthalpy, H_v	$C_{4,1}$ $C_{4,2}$ $C_{4,3}$ $C_{4,4}$
Nitrogen Vapor Enthalpy, H_N	$C_{5,1}$ $C_{5,2}$ $C_{5,3}$ $C_{5,4}$
Agent Vapor Pressure, P_v	$C_{6,1}$ $C_{6,2}$ $C_{6,3}$ $C_{6,4}$ $C_{6,5}$
Nitrogen Liquid Volume, $V_{l,N}$	$C_{7,1}$ $C_{7,2}$
Henry's Law Constant, Hen	$C_{8,1}$ $C_{8,2}$ $C_{8,3}$ $C_{8,4}$

As mixture property data is unavailable, the additional liquid volume and the Henry's Law coefficient were first estimated using the Soave-Redlich-Kwong equation of State:

$$Z^3 - Z^2 + Z\,(A - B - B^2) - A\,B = 0$$

$$A = 0.42727\left(1. + (0.48 + 1.574\,w + 0.176\,w^2)\,(1. - T_r^{0.5})\right)^2 \frac{P_r}{T_r^2} \qquad (17)$$

$$B = 0.08664\,\frac{P_r}{T_r}$$

where w is the pitzer acentric factor, T_r is the reduced temperature (T/T_c), P_r is the reduced pressure (P/P_c) and Z is the generalized compressibility. Note that the SRK equation can produce up to three zeros, with the highest and lowest values for Z corresponding to the vapor and liquid phases. The geometric mixing rules without binary interaction parameters were utilized in estimating mixture properties:

$$A_m = \Sigma\,\Sigma\,x_i\,x_j\,(A_i\,A_j)^{0.5} \qquad (18)$$

$$B_m = \Sigma\,x_i\,B_i$$

where the subscripts refer to component i or j in the mixture. The phase composition needed for the Henry's Law coefficient were estimated through the distribution coefficient, K_i, based upon mixture fugacity coefficients, ϕ, as follows:

$$K_i = \frac{y_i}{x_i} = \frac{\phi_{i,l}}{\phi_{i,v}} \qquad (19)$$

$$\phi_i = \exp\left[(Z-1)\,\frac{B_i}{B_m} - \ln(Z-B_m) - \left(\frac{A_m}{B_m}\right)\left[\left(\frac{2\,A_i^{0.5}}{A_m^{0.5}}\right) - \left(\frac{B_i}{B_m}\right)\right]\ln\frac{(Z+B_m)}{Z}\right]$$

The Rachford-Rice procedure was then employed to find the actual composition of each phase [8]. In this procedure, the fraction of the total mass in the vapor, ψ, is guessed and then iterated on until the component masses balance.

$$0 = \Sigma\,z_i\,\frac{(1 - K_i)}{1 + \psi\,(K_i - 1)} \qquad (20)$$

$$x_i = \frac{z_i}{1 + \psi\,(K_i - 1)}$$

$$y_i = x_i\,K_i$$

where z_i is the fraction of the total mass in the mixture that is component i.

5. Experimental Agreement

The flow program has been extensively tested and continues to be twted for a wide range of agents, piping networks, and flow conditions. The model has been successfully tested against experimental data for the following agents:

HFC-227ea/N_2,
FC-3-1-10/N_2,
HFC-23/N_2,
HFC-23,
HFC/HCFC/N_2 blends,
Halon 1301, and
SF_6.

The model has been compared to over 200 discharge tests and a wide range of flow conditions and piping geometries. The experimental agreement for HFC-227ea, FC-3-1-14 and Halon 1301, which were most extensively tested is as follows:

Mass flow rate:	± 10 percent,
Cylinder pressure:	± 10 percent,
Average nozzle pressure:	± 10 percent, and
Discharge time:	± 1 second.

Experimental comparison is continuing on other agents and blends. The program can be easily modified to predict flows of any HFC/HCFC/FC or halon agent or blend with or without nitrogen pressurization. The program has also been modified to calculate the flow characteristics of CF_3I based on estimated thermodynamic properties.

6. Discussion/Limitations to Model

This model in its present form has been demonstrated to predict the discharge time based on nozzle liquid runout with reasonable accuracy.

The model halts execution if the cylinder runs out of liquid prior to the liquid front reaching the last nozzle. This limit on pipe volume roughly corresponds to an NFPA 12A 70 percent agent in pipe or a pipe to initial cylinder liquid volume ratio of 160%.

The model has only been tested against two tee orientations, horizontal bull-head and horizontal side flow. There are limitations, particularly due to experimental data, on the largest flow splits that the model can handle. For both types of tees, the maximum flow split is on the order of 90 percent/10 percent.

There is no inherent limitation on the flow time imbalance between nozzles.

7. References

1. DiNenno, P.J. and Budnick, E.K., "A Review of Discharge Testing of Halon 1301 Total Flooding Systems," NFPA, Batterymarch Park, Quincy MA, 1988.

2. Elliot, D.G., Gamson, P.W., Klein, G.A., Moran, KM., and Zydowicz, M.P., "Flow of Nitrogen-Pressurized Halon 1301 in Fire Extinguishing Systems," Jet Propulsion Laboratory, Pasadena, CA, 1984.

3. Carhart, H.W., Leonard, J.T., DiNenno, P.J., Forssell, E.W., and Starchville, M.D., "Discharge System Tests of Halon 1301 Test Gas Simulants," NRL Memorandum Report 6898, Naval Research Laboratory, Washington D.C., 1991.

4. DiNenno, P.J., Forssell, E.W., Peatross, M.J., and Wong, J.T., 'Thermal Decomposition Testing of Halon 1301 Alternatives," presented at the Halon Alternatives Technical Working Conference, Albuquerque, NM, May 1993.

5. Roberson, John A. and Crowe, Clayton T., ***Engineering*** Fluid ***Mechanics,*** 2nd ***Ed,*** Houghton Mifflin Company, Boston, MA, 1980.

6. Wilson, Loren C., Wilding, W. Vincent, and Wilson, Grant M., "Thermodynamic Properties of Perfluorobutane," Wiltec Research Company, Provo, UT, 1992.

7. Reid, Robert C., Prausnitz, John M., and Sherwood, Thomas K., *The Properties of Gases and Liquids*, 3rd edition, McGraw-Hill **Book** Company, New York, ***NY,*** 1977.

8. Henley, Ernest J., and Seader, J.D., ***Equilibrium-Stage Separation Operations in Chemical Engineering,*** John Wiley and Sons, New York, ***NY,*** 1981.